Biochimica et Biophysica Acta 1832 (2013) 365–374

Contents lists available at SciVerse ScienceDirect

Biochimica et Biophysica Acta

journal homepage: www.elsevier.com/locate/bbadis

ARHGAP21 is a RhoGAP for RhoA and RhoC with a role in proliferation and migration of prostate adenocarcinoma cells

Mariana Lazarini [a,*], Fabiola Traina [a], João A. Machado-Neto [a], Karin S.A. Barcellos [a], Yuri B. Moreira [b], Marcelo M. Brandão [c], Sergio Verjovski-Almeida [b], Anne J. Ridley [d], Sara T. Olalla Saad [a,*]

[a] Hematology and Hemotherapy Center, University of Campinas/Hemocentro-Unicamp, Instituto Nacional de Ciência e Tecnologia do Sangue, INCTS, Campinas, São Paulo, Brazil
[b] Departamento de Bioquímica, Instituto de Química, Universidade de São Paulo, São Paulo, Brazil
[c] Departamento de Genética, Escola Superior de Agricultura Luiz de Queiroz, Universidade de São Paulo, Piracicaba, SP, Brazil
[d] Randall Division of Cell and Molecular Biophysics, King's College London, London, UK

ARTICLE INFO

Article history:
Received 24 May 2012
Received in revised form 15 October 2012
Accepted 16 November 2012
Available online 28 November 2012

Keywords:
ARHGAP21
RhoA
RhoC
Prostate adenocarcinoma
PC3
Endothelin-1

ABSTRACT

Background: Several Rho GTPase-activating proteins (RhoGAPs) are implicated in tumor progression through their effects on Rho GTPase activity. ARHGAP21 is a RhoGAP with increased expression in head and neck squamous cell carcinoma and with a possible role in glioblastoma tumor progression, yet little is known about the function of ARHGAP21 in cancer cells. Here we studied the role of ARHGAP21 in two prostate adenocarcinoma cell lines, LNCaP and PC3, which respectively represent initial and advanced stages of prostate carcinogenesis. Results: ARHGAP21 is located in the nucleus and cytoplasm of both cell lines and its depletion resulted in decreased proliferation and increased migration of PC3 cells but not LNCaP cells. In PC3 cells, ARHGAP21 presented GAP activity for RhoA and RhoC and induced changes in cell morphology. Moreover, its silencing altered the expression of genes involved in cell proliferation and cytoskeleton organization, as well as the endothelin-1 canonical pathway. Conclusions: Our results reveal new functions and signaling pathways regulated by ARHGAP21, and indicate that it could contribute to prostate cancer progression.

1. Introduction

ARHGAP21 is a member of the RhoGAP family of proteins that has received much attention since first being described by our group in 2002 [1–3]. RhoGAPs catalyze the conversion of active GTP-bound forms of Rho-family GTPases to their inactive GDP-bound state. Rho family GTPases are key regulators of many cell functions, including actin reorganization, migration, gene transcription, survival, adhesion, and proliferation [4,5]. Several Rho GTPases are known to contribute to cancer progression [4], with either oncogenic or tumor suppressor activities [6,7]. There are 20 human Rho GTPase genes, of which the most extensively studied members are RhoA, Rac1 and Cdc42. When activated, Rho GTPases interact with several downstream effector proteins leading to activation of multiple signaling pathways which results in cellular responses until intrinsic or RhoGAP-mediated GTPase activity returns the proteins to the GDP-bound state [8].

ARHGAP21 is a protein with 1958 amino acids that contains, in addition to the RhoGAP domain, a PDZ and a pleckstrin homology (PH) domain. It has been reported that ARHGAP21 has RhoGAP activity for RhoA and Cdc42 [9,10] and interacts with several proteins, such as FAK, PKC-ζ, α-catenin, β-arrestin-1 and ARF1, mediating cross-talk between Rho GTPases and other signaling pathways [1,3,9–11]. ARHGAP21 plays a role in the vesicular trafficking of Golgi membranes, cell–cell interactions, influenza virus replication and cardiac stress [3,9,12,13], but its function in cancer cells has been poorly investigated. ARHGAP21 is overexpressed in head and neck squamous cell carcinoma, and could be a possible potential therapeutic target [14]. We found that ARHGAP21 silencing in glioblastoma cell lines increased cell migration and secretion of metalloprotease-2, as well as FAK and Cdc42 activities [11].

Other RhoGAPs have been investigated in solid tumors, with roles in cancer development and progression, including prostate cancer [15–17]. Prostate cancer is one of the leading causes of cancer-related mortality among men worldwide [18]. Although there has been progress in the last years, several challenges remain regarding diagnosis and treatment [19]. Several signaling pathways are known to be aberrantly activated in prostate cancer progression, including the endothelin-1 pathway [20,21]. However, a better understanding of the molecular mechanisms related to prostate cancer progression may lead to more effective

* Corresponding authors at: Hematology and Hemotherapy Center, University of Campinas, Rua Carlos Chagas, 480, CEP 13083-878, Campinas, SP, Brazil. Tel.: +55 19 35218734; fax: +55 19 3289 1089.
E-mail addresses: marilazarini@gmail.com (M. Lazarini), sara@unicamp.br (S.T.O. Saad).

0925-4439/$ – see front matter © 2012 Elsevier B.V. All rights reserved.
http://dx.doi.org/10.1016/j.bbadis.2012.11.010

therapeutic strategies. We therefore aimed to evaluate ARHGAP21 functions in prostate adenocarcinoma cell lines.

2. Materials and methods

2.1. Cell culture

LNCaP and PC3 cell lines were used as a model for human prostate adenocarcinoma in specific assays as appropriated. HEK293T cells were used for pull down assays. Cell lines were obtained from ATCC (Philadelphia, PA, USA) and cultured in appropriate medium (RPMI for LNCaP and PC3 cells and DMEM for HEK293T cells) containing 10% fetal bovine serum with penicillin/streptomycin and maintained at 37 °C, 5% CO_2. HUVECs were purchased from PromoCell (Heidelberg, Germany) and cultured according to the manufacturer's instructions.

2.2. Plasmid constructs

The plasmid pCMV containing the cDNA encoding full-length human ARHGAP21 and the empty vector were purchased from OriGene Technologies (Rockville, MD, USA). The plasmids encoding pEGFP wild type RhoA, RhoC and constitutively active Cdc42 (Q61L) were provided by Ferran Valderrama (St George's, University of London). The plasmid encoding FLAG-p190-B RhoGAP in CMV2 expression vector was a kind gift from Jeff Settleman (Massachusetts General Hospital, Cambridge, USA).

2.3. Immunofluorescence and confocal microscopy

PC3 and LNCaP cells were grown on cover slips and fixed in 4% paraformaldehyde for 20 min, permeabilized with 0.5% Triton X-100 in PBS for 10 min at room temperature and blocked in PBS containing 3% bovine serum albumin (BSA) (60 min at room temperature). The cells were then incubated overnight at 4 °C with anti-ARHGAP21 antibody (sc-98336, Santa Cruz, CA, USA), diluted in PBS (1:200) containing 1% BSA, followed by incubation with secondary antibody diluted in PBS (1:400) containing 1% BSA for 2 h at room temperature. All incubations were followed by three 5-minute PBS washes. The slides were mounted in ProLong Gold Anti-Fade Mounting Medium with DAPI (Molecular Probes). Images were generated using a confocal laser-scanning microscope (LSM 510, Carl Zeiss, Welwyn Garden City, UK).

2.4. Subcellular fractionation

PC3 and LNCaP cells were trypsinized and collected by centrifugation at 200 ×g for 5 min at 4 °C. Cells were washed in ice-cold phosphate-buffered saline and collected by centrifugation at 1500 ×g for 5 min at 4 °C. The pellets were gently resuspended in buffer 1 (10 mM Hepes pH 7.9, 1.5 mM $MgCl_2$, 10 mM KCl, 0.5 mM DTT, 10 mM Na_3VO_4 and 2 mM PMSF). Cells were chilled on ice for 10 min and then lysed by the addition of 0.1% (v/v) Nonidet P-40 and homogenization by 10 passages through a 26.5-gauge needle. The extracts were centrifuged at 12.000 ×g for 10 min at 4 °C. The supernatant was used as a cytosolic and membrane fraction. The pellet was resuspended with a buffer 2 (20 mM HEPES pH 7.9, 25% Glycerol, 1.5 mM $MgCl_2$, 20 mM KCl, 0.2 mM EDTA, 0.5 mM DTT, 10 mM Na_3VO_4 and 2 mM PMSF). The homogenate was incubated on ice for 30 min at 4 °C and centrifuged at 12.000 ×g for 10 min at 4 °C. Supernatant was used as the nuclear fraction. Equal amount of proteins was used for Western blot analysis.

2.5. Transient transfections

Silencing of ARHGAP21, RhoA, RhoC and Cdc42 was performed in prostate adenocarcinoma cells using specific siRNAs from ThermoFisher Scientific (Lafayette, CO, USA), as previously described [22]. Briefly, the cells were plated at 70% confluence and transfected using Lipofectamine 2000 reagent (Invitrogen, Carlsbad, CA, USA), according to the manufacturer's instructions. Cells were analyzed 72 h after transfection. All siRNA sequences are described in Supplementary Table S1.

Overexpression of ARHGAP21, p190-B RhoGAP, GFP-RhoA and GFP-RhoC was performed with appropriated amount of vectors and jetPEI reagent (Polyplus Transfection), according to the manufacturer's instructions.

2.6. RNA extraction

Total RNA from siARHGAP21 and siControl cells was extracted using Trizol (Invitrogen), according to the manufacturer's instructions. For microarray assays, RNA was purified with Qiagen®, RNeasyTM Micro Kit and integrity of the RNAs was analyzed with Agilent 2100 Eletrophoresis Bioanalyser (Agilent Technologies, Santa Clara, CA).

2.7. Quantitative RT-PCR analysis (qPCR)

Reverse transcription reaction was performed using RevertAid™ First Strand cDNA Synthesis Kit, according to the manufacturer's instructions (MBI Fermentas, St. Leon-Rot, Germany). Real-time detection of *ARHGAP21* amplification was performed in 7500 Real-Time PCR System (Applied Biosystems) using Power SybrGreen PCR Master Mix (Applied Biosystems) and specific primers: forward 5′-ATGCACTGTACACTCGCTTCGA-3′ and reverse 5′-CAACGACGCCAGC AAAAAC-3′. *HPRT* was used as housekeeping gene and the sequence of used primers was: forward 5′-GAACGTCTTGCTCGAGATGTGA-3′, and reverse 5′-TCCAGCAGGTCAGCAAAGAAT-3′. Relative levels of gene expression were calculated using the equation, $2^{-\Delta\Delta CT}$ [23]. A negative 'No Template Control' was included for each primer pair. Three replicas were run on the same plate for each sample.

2.8. Western blotting

Cells were lysed in ice-cold Tris–HCl buffer (100 mM Tris, pH 7.5), containing 10 mM EDTA, 10% Triton X, 100 mM NaF and phosphatase and protease inhibitors (10 mM Na_3VO_4, 10 mM $Na_4P_2O_7$, 25 mM PMSF and 0.1 mg/mL aprotinin). Equal amounts of cell lysates were subjected to SDS-PAGE and western blot analysis with specific antibodies and ECL (Amersham Pharmacia Biotech, UK Ltd., Buckinghamshire, England). Polyclonal antibodies against ARHGAP21 (sc-98336), RhoA (sc-179), RhoC (sc-12116) and monoclonal antibodies against Stathmin (sc-55531) and GFP (sc-7383) were from Santa Cruz Biotechnology (Santa Cruz, CA, USA). Monoclonal antibody against p190-B RhoGAP (611612) was from BD Transduction Laboratories (San Diego, CA, USA) and polyclonal anti-Cdc42 (2462) was from Cell Signaling Technology (Danvers, MA, USA). Quantitative analyses of the optical intensities of protein bands were carried out with Un-Scan-It Gel 6.1 (Silk Scientific Inc., Utah, USA) and normalized to GAPDH or actin for protein expression or total protein for pulldown assays.

2.9. Analysis of cell proliferation

Cell proliferation was measured by methylthiazoletetrazolium (MTT) assay. Twenty-four hours after transfection, 9×10^3 cells per well were plated in a 96-well plate in RPMI containing 10% FBS. To evaluate cell viability, 10 μL of a 5 mg/mL solution of MTT (Sigma-Aldrich; St. Louis, MO, USA) were added to the wells and incubated at 37 °C for 4 h. The reaction was stopped by using 100 μL of 0.1 N HCl in anhydrous isopropanol and the absorbance was measured at 570 nm, using an automated plate reader. All conditions were tested in six replicates.

2.10. TUNEL assay

Twenty-four hours after transfection, a total of 3×10^4 cells per well were plated in a 12-well plate in RPMI containing 10% FBS. The

cells were then collected and apoptosis was evaluated by TUNEL assays using APO-BrdU™ TUNEL Assay Kit from Invitrogen, according to the manufacturer's guidelines.

2.11. Analysis of cell migration

Migration of PC3 and LNCaP cells was followed by time lapse microscopy. Twenty-four hours after siRNA transfection, 7000 cells in RPMI containing 10% FBS were plated in a 24-well plate previously coated with 100 μg/mL Matrigel (BD Biosciences, NJ, USA), 10 μg/mL fibronectin (Sigma-Aldrich), or uncoated (plastic). On the next day, the medium was changed to RPMI containing 1% FBS. Time-lapse movies were acquired using a Nikon TE2000-E microscope and a Plan Fluor 10× objective (Nikon, Kingston, UK) and a Hamamatsu Orca-ER digital camera. Image series were captured at 37 °C and 5% CO_2 at 1 frame/5 min for 17 h with Metamorph software (Molecular Devices, Wokingham, UK). Cells were tracked and migration speed was determined using ImageJ analysis software (http://rsb.info.nih.gov/ij).

2.12. Transendothelial cell migration assay

HUVECs were grown to confluence on fibronectin-coated plates. PC3 cells (4×10^4/well) in RPMI containing 10% FBS were added to the HUVECs, and time-lapse images were acquired every 3 min for 7 h as described above but with a 20× objective. Cells were tracked and the percentage of intercalation was determined using ImageJ analysis software.

2.13. GTPase activity assays

GST-WASP-RBD and GST-Rhotekin-RBD were purified from *Escherichia coli* as previously described [24]. GST-WASP-RBD pull-down assays were used to evaluate the activity of Cdc42, whereas GST-Rhotekin-RBD pull-down assays were used to evaluate RhoA and RhoC activities. Cells (10^7/pull-down) were lysed in 1 mL GST-Fish buffer (25 mM Hepes, pH 7.5, 150 mM NaCl, 1% Nonidet P-40, 10 mM $MgCl_2$, 1 mM EDTA, 25 mM NaF, 1 mM Na_3VaO_4, 10 μg/mL aprotinin, 100 μM PMSF, and 10% glycerol). Some lysate (40 μL) was retained to determine total GTPase levels. The remaining lysate was incubated with the protein-bound beads on a rotor for 2 h at 4 °C. The beads were washed three times in pull-down buffer, boiled in Laemmli sample buffer, and analyzed by western blotting.

2.14. Microarray experiments and data analysis

Gene expression measurements were performed using Whole Human Genome Oligo Microarray 4×44k with RNA obtained from three independent transfections on PC3 cells. For each individual sample, 500 ng of total RNA were amplified and labeled with Cy3 or Cy5 using the Agilent Low RNA Input Fluorescent Linear Amplification Kit PLUS, two-Color (Agilent Technologies) according to the manufacturer's recommendations. Labeled cRNA was hybridized using Gene Expression Hybridization Kit (Agilent). Slides were washed and processed according to the Agilent Two-Color Microarray-Based Gene Expression Analysis protocol (Version 5.5) and scanned on a GenePix 4000 B scanner (Molecular Devices, Sunnyvale, CA, USA). Fluorescence intensities were extracted using Feature Extraction (FE) software (version 9.0; Agilent). Genes differentially expressed between siControl and siARHGAP21 were identified with the Significance Analysis of Microarray (SAM) statistical approach [25], using the following parameters: one-class unpaired responses, t-statistic, 16 permutations. False discovery rate (FDR) was 15%. The list of altered genes was uploaded to Ingenuity Pathways Analysis (IPA) software (IngenuityR Systems, http://www.ingenuity.com) for the identification of relevant altered gene networks and canonical gene pathways. The raw data has been deposited in Gene Expression Omnibus (GEO) http://www.ncbi.nlm.nih.gov/geo/ database under accession number GSE37888. All gene annotations were performed using Blast2GO [26].

2.15. Statistical analysis

Statistical analysis was performed using GraphPad Instat 5 (GraphPad Software, Inc., San. Diego, CA, USA). Data were expressed as the mean ± SD. For comparisons, an appropriate Student's *t*-test was used. The level of significance was set at $p<0.05$.

3. Results

3.1. ARHGAP21 localizes in the nucleus and cytoplasm of PC3 and LNCaP cells

Since ARHGAP21 expression and localization have never been evaluated in prostate adenocarcinoma cell lines, we first evaluated ARHGAP21 localization in PC3 and LNCaP cells by immunofluorescence. ARHGAP21 was expressed and had a nuclear and cytoplasmic localization in both cell lines, with prominent perinuclear localization. Interestingly, ARHGAP21 also localized in protrusions of PC3 and LNCaP cells (Fig. 1A). The staining intensity with the ARHGAP21 antibody was lower in cells depleted of ARHGAP21 by RNAi, indicating the specificity of the antibody (Supplementary material, Fig. S1). ARHGAP21 nuclear and cytoplasmic localization in PC3 and LNCaP cells was confirmed by cell fractionation and western blotting. The efficacy of the fractionation protocol was verified by subcellular distribution of the cytoplasmic protein stathmin and of the nuclear protein histone H4 (Fig. 1B).

3.2. ARHGAP21 silencing reduces proliferation but not apoptosis in prostate cancer cells

PC3 and LNCaP cells silenced for ARHGAP21 (siARHGAP21) (Fig. 2A) were used to investigate the function of ARHGAP21 in prostate adenocarcinoma.

Rho GTPases are well known to affect cell proliferation [4]. The effect of ARHGAP21 on the proliferation of PC3 and LNCaP cells was therefore determined. Proliferation was significantly reduced in ARHGAP21-depleted PC3 cells compared to control cells, whereas no difference was observed in LNCaP cells (Fig. 2B). The decrease in PC3 cell number was not due to increased apoptosis, since the % of apoptotic cells did not differ between siControl and siARHGAP21-transfected PC3 or LNCaP cell lines (Fig. 2C).

3.3. ARHGAP21 silencing increases PC3 cell migration on fibronectin but does not affect interaction with endothelial cells

Rho GTPases regulate cell migration, and thus we investigated whether ARHGAP21 knockdown affected cell motility. PC3 and LNCaP cells were plated onto 3 different substrates: uncoated plastic or Matrigel or fibronectin coated-dishes. We observed an increase in the migration speed of ARHGAP21-depleted PC3 cells specifically on fibronectin, compared to control cells (0.33 ± 0.22 and 0.39 ± 0.22 μm/min for PC3 siControl and siARHGAP21, respectively; $p<0.05$). There was no difference in their migration speed on plastic or Matrigel (Fig. 3A). ARHGAP21 depletion did not alter the migration speed of LNCaP cells under any of the conditions tested (data not shown).

Cancer metastasis involves interaction of cancer cells with endothelial cells [27]. As previously described [28], we observed that PC3 cells rapidly insert (intercalate) into a monolayer of HUVECs: approximately 55% of PC3 cells intercalate by 1 h and 95% by 7 h (Supplementary material, Fig. S2). However, ARHGAP21 depletion did not alter the timecourse of PC3 cell intercalation (Fig. 3B). Our results indicate that ARHGAP21 specifically affects migration speed of PC3 cells but not interaction with endothelial cells.

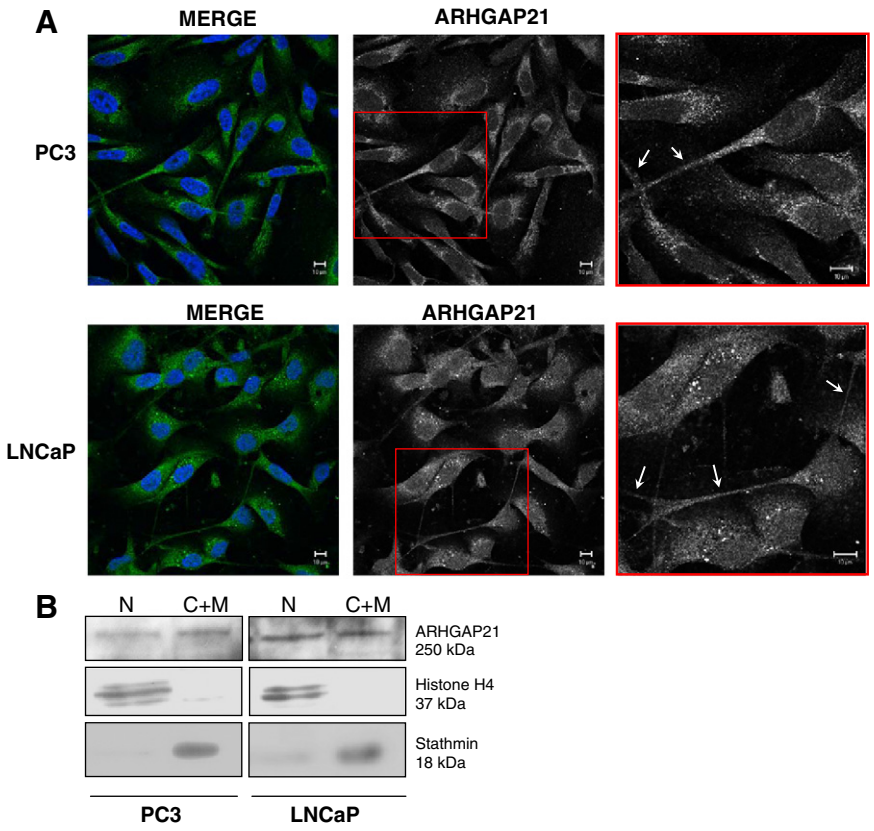

Fig. 1. ARHGAP21 localization in prostate adenocarcinoma cell lines. (A) Confocal micrographs of PC3 and LNCaP cell lines stained for ARHGAP21 (green) and with DAPI (blue). Note that ARHGAP21 localizes in the nucleus, cytoplasm and cell protrusions (white arrows) of both cell lines. Scale bar, 10 μm. (B) Cell fractionation of PC3 and LNCaP cell lines, which confirms the cytoplasmic and nuclear localization of ARHGAP21. The efficiency of the fractionation was verified by stathmin and histone H4 blots, which are respectively localized in the cytoplasm and nucleus. N = nuclei; C + M = cytoplasm and membrane.

3.4. ARHGAP21 has GAP activity for RhoA and RhoC and induces morphological changes in PC3 cells

Previous studies have shown that ARHGAP21 acts as a RhoGAP protein for RhoA and Cdc42 [9,12]. Given that RhoGAP specificity can vary between in vitro and in vivo assays and that ARHGAP21 has never been tested for RhoC, we measured the effects of ARHGAP21 silencing and overexpression on RhoA, RhoC and Cdc42 activities in PC3 cells.

ARHGAP21 silencing increased RhoA and RhoC activity compared to control cells but, surprisingly, no difference in Cdc42 activity was observed (Fig. 4A). Corroborating these findings, ARHGAP21 overexpression decreased RhoA and RhoC activities, but not Cdc42 (Fig. 4B). Cells silenced for RhoA, RhoC or Cdc42, cells overexpressing p190-B RhoGAP, which is known to act as a GAP for RhoA [17], and cells overexpressing GFP-Cdc42-L61 were used as internal controls of Rho GTPase activity assays, as indicated (Fig. 4A–B). The efficiency of ARHGAP21 and p190-B RhoGAP overexpression is shown in Fig. 4C.

Interestingly, ARHGAP21 overexpression induced similar morphological changes to p190-B RhoGAP in PC3 cells, characterized by cell rounding, increase in the number and length of protrusions and detachment from the tissue culture plastic plate (Fig. 4D). This is consistent with ARHGAP21 acting predominantly as a RhoA/RhoC GAP in PC3 cells. ARHGAP21 overexpression in HEK293T cells resulted in similar effects on RhoA, RhoC and Cdc42 activities and cell morphology (Supplementary material, Fig. S3).

In order to investigate whether the effects of ARHGAP21 silencing effects were due to elevated RhoA and RhoC activities, we further investigated the effect of GFP-RhoA or GFP-RhoC overexpression (Fig. 5A) on proliferation and migration of PC3 cells. In contrast to ARHGAP21 silencing, both RhoA and RhoC overexpression slightly increased proliferation of PC3 cells (Fig. 5B), which is in accordance with the previous studies [29–31]. Similar to ARHGAP21 silencing, GFP-RhoC overexpression increased migration speed compared to control, in agreement with other reports [31]. Overexpression of GFP-RhoA did not alter the migration speed of PC3 cells on fibronectin (Fig. 5C). These results indicate that the effect of ARHGAP21 silencing on migration is most likely due to increased RhoC activity, whereas the effects on proliferation are probably caused by effects on other signaling pathways and not RhoA or RhoC.

3.5. ARHGAP21 alters gene expression in PC3 cells

To investigate other signaling pathways that could be modulated by ARHGAP21 and contribute to the observed phenotypes of ARHGAP21-depleted cells, gene expression was analyzed with Whole Human Genome Oligo Microarrays (Agilent Technologies) using RNA from siARHGAP21-depleted and siControl-transfected PC3 cells. A total of 110 differentially expressed genes between siARHGAP21 and siControl were identified: 93 were down-regulated and 17 up-regulated in siARHGAP21-depleted cells (Supplementary Fig. S3). The signature expression profile revealed genes related to several biological processes, including cell proliferation and cytoskeleton organization (Table 1). Using Ingenuity Pathways Analysis (IPA), we identified 7 relevant networks that were significantly enriched ($p<0.001$) with the genes altered in ARHGAP21-depleted PC3 cells. A gene network involved in cellular development, cellular growth and proliferation and connective tissue development and function is represented in Fig. 6A. Of the top canonical

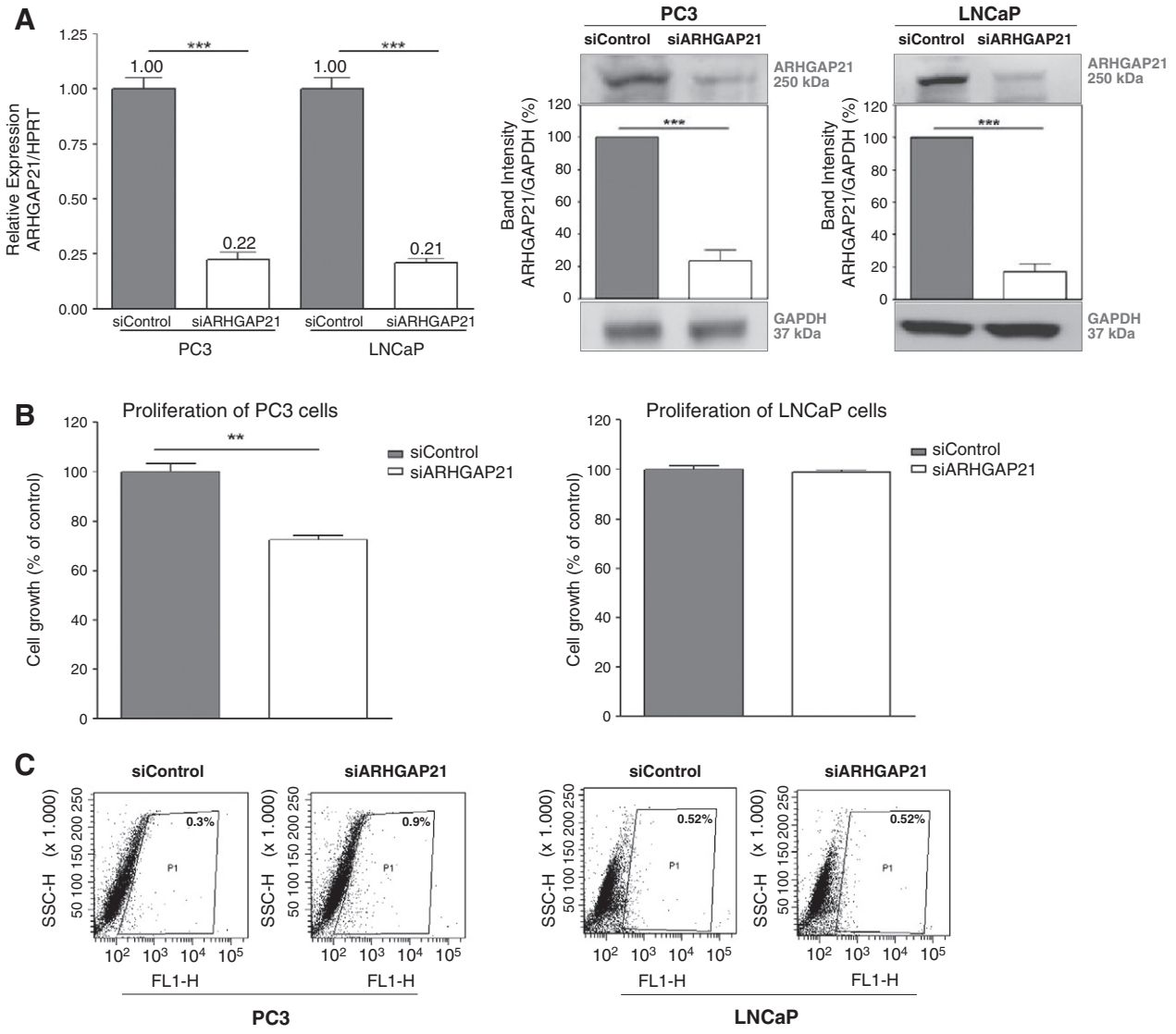

Fig. 2. ARHGAP21 silencing affects proliferation of PC3 but not LNCaP cells. (A) PC3 and LNCaP cells were transfected with siARHGAP21 or siControl. Cells were analyzed after 72 h. Left, Quantitative analysis of *ARHGAP21* mRNA expression. mRNA expression levels of *ARHGAP21* were normalized to *HPRT* endogenous control and were analyzed by qPCR using $2^{-\Delta\Delta CT}$. Data shown are the mean ± SD of 3 independent experiments. ***p<0.001; two-way Student's *t*-test. Right, western blotting analysis of total cell extracts, probed with antibodies against ARHGAP21 (250 kDa), or GAPDH (37 kDa) as a loading control. Data shown are the mean ± SD of three replicates and are representative of 3 independent experiments. ***p<0.001; two-way Student's *t*-test. (B) Cell proliferation was determined by MTT assay. Data shown are the mean ± SD of six replicates and are representative of 3 independent experiments. **p<0.01; two-way Student's *t*-test. (C) Apoptosis was detected by flow cytometry using TUNEL staining. The gate (P1) contains the apoptotic population. The % of apoptotic cells is shown. Results are representative of 3 independent experiments.

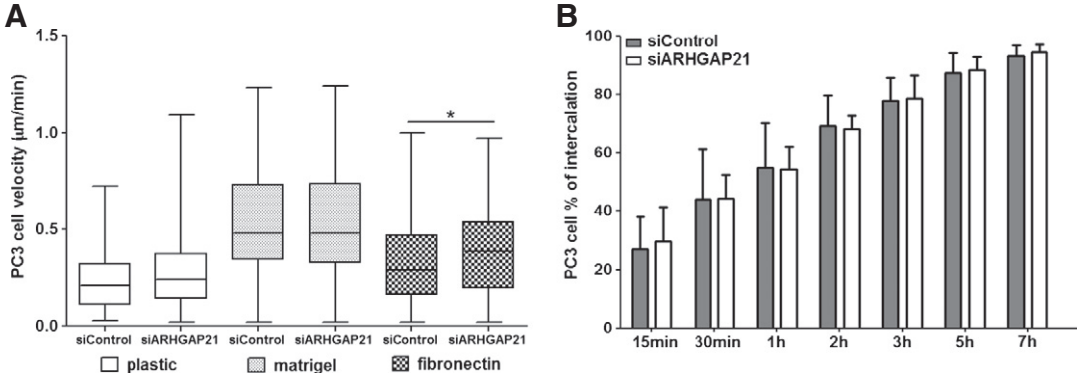

Fig. 3. Effects of ARHGAP21 silencing on PC3 cell migration and endothelial interaction. PC3 cells were transfected with siARHGAP21 or siControl as indicated. (A) Migration assays on uncoated plastic (plastic), or plastic coated with Matrigel or fibronectin. Cell migration speed was determined from time-lapse movies. Box and whisker plots of speed: the central boxes represent values from the lower to upper quartile (25th to 75th percentiles), the middle line indicates median and the vertical line extends from the minimum to maximum values. Three separate experiments were performed and at least 40 cells from each experiment were analyzed by two-way unpaired Student's *t*-test, *p<0.05. (B) PC3 cells were plated on a HUVEC monolayer. The percentage of intercalated PC3 cells at different timepoints was determined by time-lapse microscopy. Data shown are the mean of 4 independent experiments ± SD. At least 100 cells were analyzed in each experiment; two-way unpaired Student's *t*-test showed no significant differences.

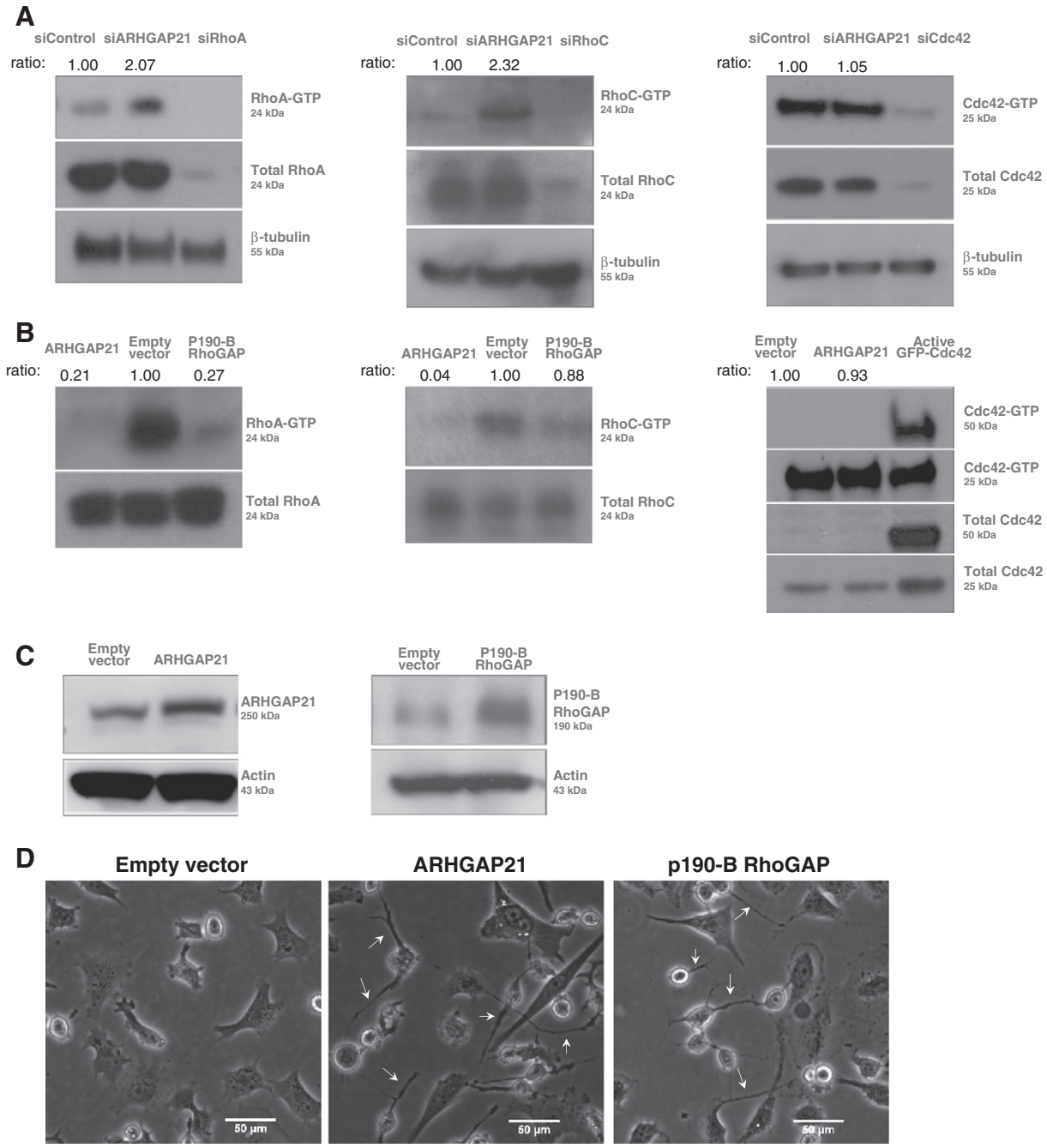

Fig. 4. ARHGAP21 regulates RhoA and RhoC activity. GST-Rhotekin-RBD pull down assays were performed to evaluate RhoA and RhoC activities, and GST-WASP-PBD pull down assays were used to determine Cdc42 activity. Assays were performed in PC3 cells silenced for ARHGAP21 (A) or overexpressing ARHGAP21 (B). PC3 cells silenced for RhoA, RhoC or Cdc42 or cells overexpressing p190-B RhoGAP or GFP-Cdc42-L61 were used as controls for the assay efficiencies, as indicated. Protein extracts from pull down and total protein were used for western blot assays and blotted with the antibodies anti-RhoA (left), RhoC (middle) or Cdc42 (right). Densitometry was performed and a ratio of active protein versus total protein compared with the normalized value of control is shown. (C) Western blot analysis of total extracts from PC3 cells transfected with empty vector, or vectors encoding ARHGAP21 (left panel) or p190-B RhoGAP (right panel). The efficiency of transfections was evaluated with antibodies against ARHGAP21 (250 kDa), p190-B RhoGAP (190 kDa) or Actin (43 kDa), as a loading control. (D) Morphology of PC3 cells after transfection with empty vector, or vectors encoding ARHGAP21 or p190-B RhoGAP. ARHGAP21 and p190-B RhoGAP expression resulted in cell rounding and formation of protrusions, indicated by white arrows. Scale bars, 50 μm.

pathways statistically modulated in PC3 cells silenced for ARHGAP21 ($p<0.005$), we detected endothelin-1 signaling, known to regulate cell proliferation and migration [32] (Fig. 6B). Interestingly, we also observed statistically significant modulation of the canonical pathway named Role of MAPK Signaling in the Pathogenesis of Influenza (data not shown), which is related to the study performed by Wang et al., who observed lower rates of influenza virus replication in a human alveolar epithelial cell line silenced for ARHGAP21 [13].

4. Discussion

We have investigated the function of the RhoGAP ARHGAP21 in prostate adenocarcinoma cell lines. We observed that ARHGAP21 localizes in the nucleus, cytoplasm and cell protrusions of both PC3 and LNCaP cells, with a prominent localization in the perinuclear region. Previous work from our group showed a nuclear and perinuclear localization of ARHGAP21 in different cell lines [11]. Moreover, other studies showed

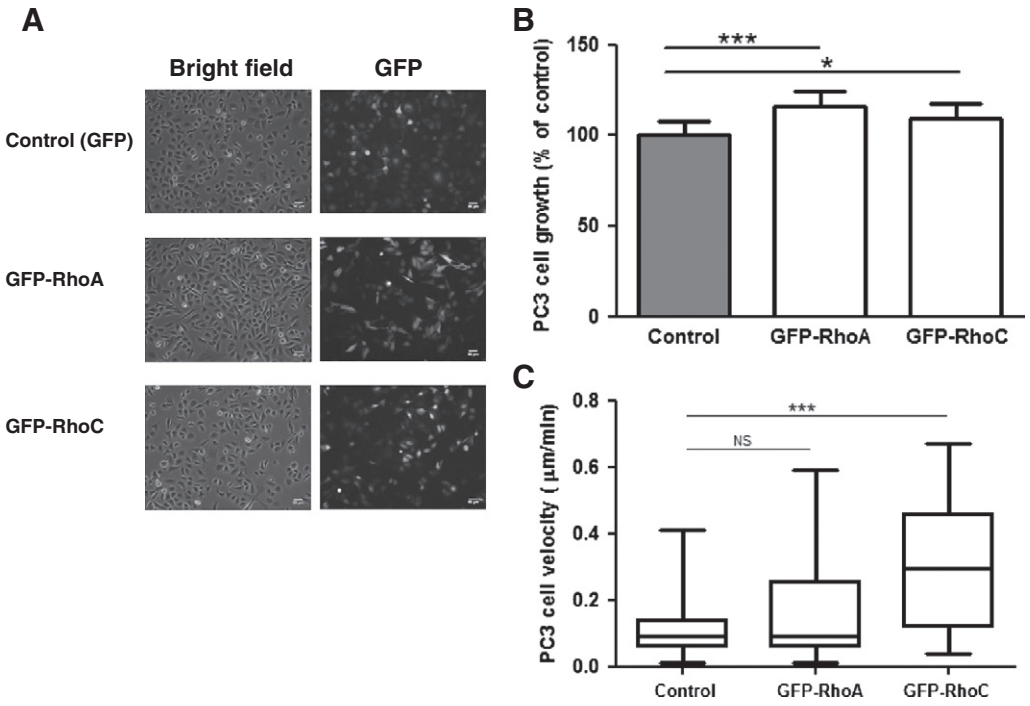

Fig. 5. Effects of RhoA and RhoC overexpression on PC3 cell proliferation and migration. (A) PC3 cells were transfected with indicated vectors and transfection efficiency was evaluated by detecting green fluorescent protein (GFP) by fluorescence microscopy. (B) MTT assays in cells cultured in 10% FBS. Data shown are the mean ± SD of six replicates and are representative of 3 independent experiments. ***$p<0.01$; *$p<0.05$; two-way Student's *t*-test. (C) Migration assays on fibronectin. Cell migration speed was determined from time-lapse movies. Box and whisker plots of speed: the central boxes represent values from the lower to upper quartile (25th to 75th percentiles), the middle line indicates median and the vertical line extends from the minimum to maximum values. Three separate experiments were performed and at least 40 cells from each experiment were analyzed by two-way unpaired Student's *t*-test, NS = not significant ($p>0.05$); ***$p<0.001$.

a Golgi-specific localization in HeLa and MCF-7 cells [9,12] and cytoplasmic localization in head and neck squamous carcinomas [14]. We hypothesize that different cell types and tissues may have different patterns of ARHGAP21 localization, reflecting their specific characteristics and functions.

LNCaP and PC3 cell lines are commonly used as representative of prostate cancer. Both cell lines retain the expression of the prostate specific antigen (PSA) [33]; however, they have different responses to hormones [34] and diverge in the expression of other prostate cancer markers [35–37]. Whereas LNCaP cells represent an initial androgen-responsive stage of prostate cancer, PC3 cells are characterized by a more aggressive behavior [38]. Interestingly, our results showed that ARHGAP21 only affected proliferation and migration of PC3 but not LNCaP cells, suggesting that ARHGAP21 has a more dominant role in cells from an advanced stage of prostate cancer, and that increased ARHGAP21 expression would stimulate prostate cancer proliferation. We thus focused our attention on the PC3 cell line model.

Table 1
Biological processes of genes differentially expressed in PC3 siARHGAP21.

Biological process[a]	Genes differentially expressed
Response to stress	↓GP6, ↓PLA2G4C, ↓W60781, ↓ATRX, ↓C5, ↓FCMD, ↓SAA4, ↓DCN, ↓CCL20, ↓IL1A, ↓IL29, ↓PTGS2, ↓UTS2, ↓RDM1, ↓TFF3, ↓PLA2G7, ↓PLA2G4A, ↓STX4, ↓ENDRA, ↑NF1, ↑HMOX1, ↑AXL
Transport	↓PLA2G4C, ↓STX4, ↓SYNE2, ↓ENDRA, ↑HMOX1, ↓UPK1A, ↑APOL6, ↑SLC20A1, ↑AXL, ↑NF1, ↓TCN1, ↓SLC5A6, ↑RAB15, ↓UTS2, ↓NLGN1, ↓C5
Cell differentiation	↓IL29, ↓ENDRA, ↓IL1A, ↓UPK1A, ↓TCP11, ↓SEMA3C, ↑AXL, ↑NF1, ↓W60781, ↓SPINK5, ↑NEURL, ↓UTS2, ↓BMP3, ↓NLGN1, ↓ETV1
Cell proliferation	↑AXL, ↑NF1, ↓W60781, ↓CDC25A, ↓UTS2, ↓PLA2G7, ↓FCMD, ↓IL29, ↓ENDRA, ↑CNTD2, ↑HMOX1, ↓IL1A, ↓PTGS2, ↓NOX5
Cell death	↓C5, ↓PLA2G7, ↓ENDRA, ↑HMOX1, ↓IL1A, ↓PTGS2, ↓NOX5, ↑AXL, ↑NF1, ↓GRID2
Cell–cell signaling	↓CCL20, ↓PTGS2, ↑NF1, ↑RAB15, ↓UTS2, ↓BMP3, ↓NLGN1, ↓STX4, ↓GRID2
Cell cycle	↓HPGD, ↓CDC25A, ↓PFTK1, ↓MAP3K8, ↓CKS2, ↓IL1A, ↓PTGS2, ↑CNTD2
Anatomical structure morphogenesis	↓DCN, ↓SEMA3C, ↑AXL, ↑SOX13, ↑NF1, ↓SPINK5, ↑NEURL, ↓UTS2, ↓ETV1, ↓C5, ↓ENDRA, ↑HMOX1, ↓IL1A, ↓PTGS2, ↓NOX5
Cytoskeleton organization	↑NF1, ↑NEURL, ↓CKS2

[a] The biological processes categories were obtained from the Blast2GO database. Genes (↑) up-regulated or (↓) down-regulated in ARHGAP21-depleted PC3 cells with respect to control PC3 cells.

We found that ARHGAP21 overexpression decreased both RhoA and RhoC activities. Most RhoGAPs have only been tested on RhoA but not RhoC. Despite their high level of homology, RhoA and RhoC have different functions and can act through distinct effectors [22,39,40]. RhoA frequently decreases whereas RhoC enhances cancer cell migration and invasion [41,42], and RhoC is up-regulated during epithelial–mesenchymal transition, concomitant to a decrease of RhoA activation [43]. Surprisingly, we observed no changes in Cdc42 activity in PC3 or HEK293T cells. Previous studies from our group showed an increase in Cdc42 activity upon ARHGAP21 silencing in a glioblastoma cell line [11]. We hypothesize that the ARHGAP21 specificity for different Rho GTPases may vary according to the cell type, which could be related to its specific localization [44]. Our results suggest that the increased migration observed by ARHGAP21 depletion may be due to increased RhoC activity, as both ARHGAP21 silencing and RhoC overexpression increased PC3 cell migration on fibronectin. Moreover, our results indicate that the phenotypic effects of ARHGAP21 overexpression in PC3 and HEK293T cells are mostly due to RhoA/RhoC, as the shape change was similar to that induced by p190-B RhoGAP, which acts on RhoA and RhoC (our work) but not Cdc42 [45,46]. A similar phenotype induced by p190 RhoGAP expression in fibroblasts has already been described and was associated with the down-regulation of RhoA activity, since expression of constitutively activated RhoA suppressed the phenotype [47,48].

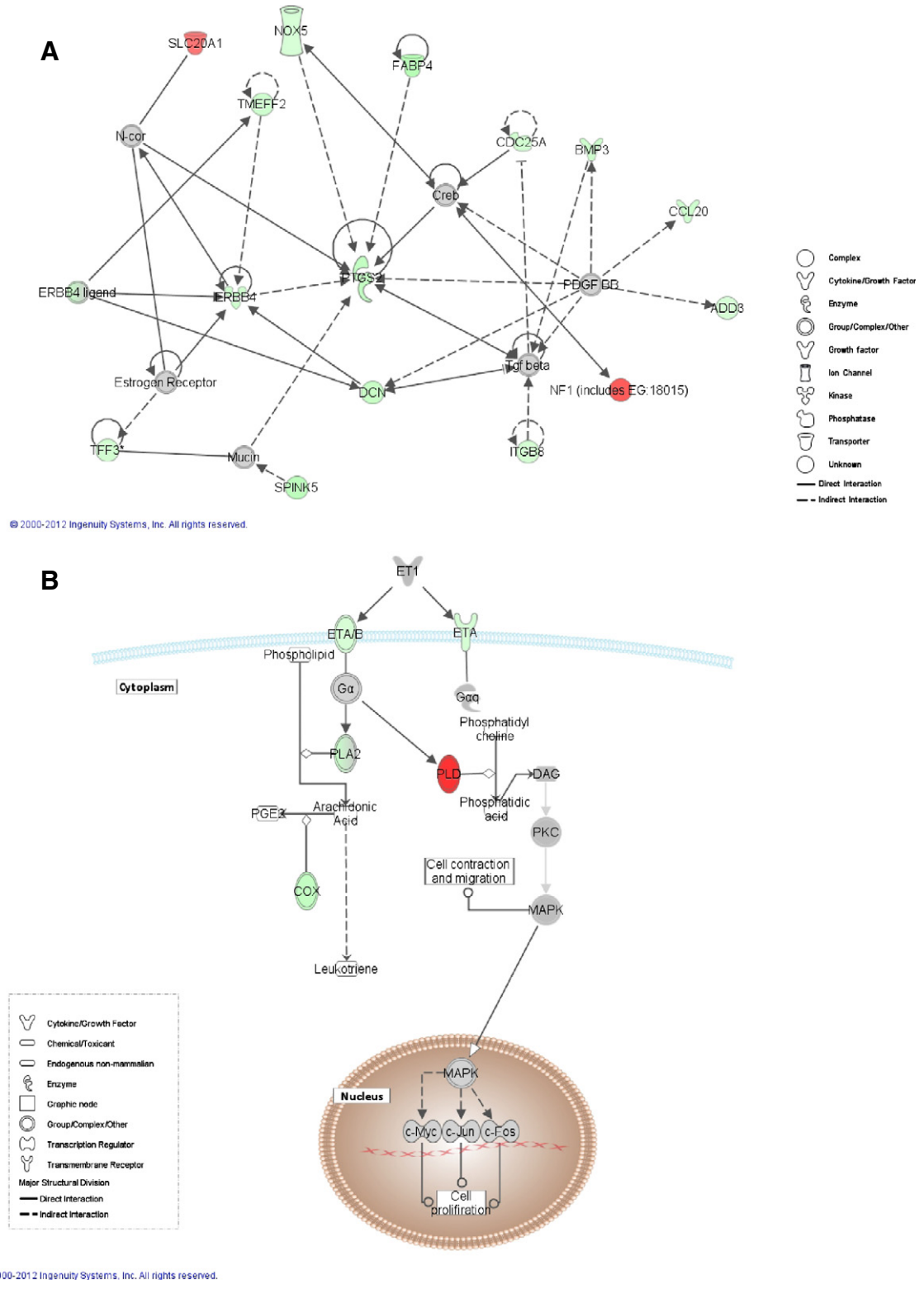

Fig. 6. Pathway Analysis of gene expression changes induced by ARHGAP21 depletion. (A) Ingenuity Pathways Analysis identified that the top most significantly enriched ($p<0.001$) network contained genes that are related to cellular development, growth and proliferation and connective tissue development and function. (B) Ingenuity Pathways Analysis identified that the endothelin-1 canonical pathway was significantly enriched ($p<0.001$) with altered genes. Gene color intensity indicates the degree of up-regulation (red) or of down-regulation (green) in siARHGAP21-transfected PC3 cells in comparison to siControl-transfected cells. Genes in gray were either not detected as expressed or not modulated by ARHGAP21 silencing in these cells.

On the other hand, ARHGAP21 silencing effects on proliferation were opposite to the effects of RhoA and RhoC overexpression, which lead us to investigate other signaling pathways related to ARHGAP21. The fact that there are more than 70 RhoGAPs for only 20 Rho GTPases and that each of them has one or more additional domains indicates that RhoGAPs do not function simply as regulators of Rho GTPases.

Indeed, several ARHGAP21 partners have been already described, such as FAK, PKC-ζ, α-catenin, β-arrestin-1 and ARF1 [1,3,9–11], indicating that ARHGAP21 is a scaffolding protein in addition to a GAP. In this study, we found that ARHGAP21 silencing modulated the expression of several genes, including genes belonging to the endothelin-1 signaling pathway.

Endothelin-1 is well-known to increase actomyosin contractility and is involved in many cell functions [49]. Activation of endothelin-A receptor by endothelin-1 promotes cell proliferation [20,50–52] and there is accumulating evidence that selective blocking of this receptor may be useful in prostate cancer treatment [53–55]. The decrease in PC3 cell proliferation upon ARHGAP21 depletion could therefore be related to its modulation of the endothelin-1 pathway, especially the down-regulation of endothelin-A receptor observed in our microarray results. Previous studies have showed that ARHGAP21 partners are involved with the endothelin-1 pathway. Endothelin-1 induces RhoA and FAK activation [56,57]. Interestingly, ARHGAP21 has recently been described as a partner of β-arrestin 1 and this interaction is increased upon angiotensin II stimulation, regulating RhoA activation [1]. β-arrestin 1 was described to be recruited by the endothelin-A receptor, and its silencing resulted in regulation of endothelin-A receptor-driven signaling in ovarian cancer cells [58].

In conclusion, our results indicate that, in PC3 prostate adenocarcinoma cells, ARHGAP21 modulates cell proliferation and migration, and expression of genes related to proliferation, cytoskeleton organization, and the endothelin-1 canonical pathway. Moreover, we showed that ARHGAP21 has GAP activity for RhoA and RhoC and its overexpression induces phenotypic changes consistent with inhibition of RhoA/RhoC. Taken together, our study points to a role of ARHGAP21 in aggressive prostate cancer and thus it will be interesting to investigate whether its expression correlates with prostate cancer progression in the future.

Acknowledgements

We thank Dr. Mariana Ozello Baratti for valuable technical assistance with the microarray assays, Dr. Ferran Valderrama for helping with the timelapse microscopy and for providing the wild type GFP-RhoA and GFP-RhoC and for the GFP-Cdc42-L61 constructs. We also thank Dr. Philippe Riou for helping with Rho activity assays. This work was supported by Conselho Nacional de Desenvolvimento Científico e Tecnológico (CNPq), Fundação de Amparo à Pesquisa do Estado de São Paulo (FAPESP), and Cancer Research UK. The Haematology and Haemotherapy Centre–UNICAMP forms part of the National Institute of Blood, Brazil (INCT de Sangue–CNPq/MCT).

Appendix A. Supplementary data

Supplementary data to this article can be found online at http://dx.doi.org/10.1016/j.bbadis.2012.11.010.

References

[1] D.F. Anthony, Y.Y. Sin, S. Vadrevu, N. Advant, J.P. Day, A.M. Byrne, M.J. Lynch, G. Milligan, M.D. Houslay, G.S. Baillie, beta-Arrestin 1 inhibits the GTPase-activating protein function of ARHGAP21, promoting activation of RhoA following angiotensin II type 1A receptor stimulation, Mol. Cell. Biol. 31 (2011) 1066–1075.
[2] D.S. Basseres, E.V. Tizzei, A.A. Duarte, F.F. Costa, S.T. Saad, ARHGAP10, a novel human gene coding for a potentially cytoskeletal Rho-GTPase activating protein, Biochem. Biophys. Res. Commun. 294 (2002) 579–585.
[3] L. Borges, C.L. Bigarella, M.O. Baratti, D.P. Crosara-Alberto, P.P. Joazeiro, K.G. Franchini, F.F. Costa, S.T. Saad, ARHGAP21 associates with FAK and PKCzeta and is redistributed after cardiac pressure overload, Biochem. Biophys. Res. Commun. 374 (2008) 641–646.
[4] F.M. Vega, A.J. Ridley, Rho GTPases in cancer cell biology, FEBS Lett. 582 (2008) 2093–2101.
[5] S. Etienne-Manneville, A. Hall, Rho GTPases in cell biology, Nature 420 (2002) 629–635.
[6] A.B. Jaffe, A. Hall, Rho GTPases: biochemistry and biology, Annu. Rev. Cell Dev. Biol. 21 (2005) 247–269.
[7] A. Hakem, O. Sanchez-Sweatman, A. You-Ten, G. Duncan, A. Wakeham, R. Khokha, T.W. Mak, RhoC is dispensable for embryogenesis and tumor initiation but essential for metastasis, Genes Dev. 19 (2005) 1974–1979.
[8] A.L. Bishop, A. Hall, Rho GTPases and their effector proteins, Biochem. J. 348 (Pt. 2) (2000) 241–255.
[9] S. Sousa, D. Cabanes, C. Archambaud, F. Colland, E. Lemichez, M. Popoff, S. Boisson-Dupuis, E. Gouin, M. Lecuit, P. Legrain, P. Cossart, ARHGAP10 is necessary for alpha-catenin recruitment at adherens junctions and for *Listeria* invasion, Nat. Cell Biol. 7 (2005) 954–960.
[10] T. Dubois, O. Paleotti, A.A. Mironov, V. Fraisier, T.E. Stradal, M.A. De Matteis, M. Franco, P. Chavrier, Golgi-localized GAP for Cdc42 functions downstream of ARF1 to control Arp2/3 complex and F-actin dynamics, Nat. Cell Biol. 7 (2005) 353–364.
[11] C.L. Bigarella, L. Borges, F.F. Costa, S.T. Saad, ARHGAP21 modulates FAK activity and impairs glioblastoma cell migration, Biochim. Biophys. Acta 1793 (2009) 806–816.
[12] T. Dubois, P. Chavrier, ARHGAP10, a novel RhoGAP at the cross-road between ARF1 and Cdc42 pathways, regulates Arp2/3 complex and actin dynamics on Golgi membranes, Med. Sci. (Paris) 21 (2005) 692–694.
[13] S. Wang, H. Li, Y. Chen, H. Wei, G.F. Gao, H. Liu, S. Huang, J.L. Chen, Transport of influenza A virus neuraminidase (NA) to host cell surface is regulated by ARHGAP21 and Cdc42, J. Biol. Chem. 287 (2012) 9804–9816.
[14] A. Carles, R. Millon, A. Cromer, G. Ganguli, F. Lemaire, J. Young, C. Wasylyk, D. Muller, I. Schultz, Y. Rabouel, D. Dembele, C. Zhao, P. Marchal, C. Ducray, L. Bracco, J. Abecassis, O. Poch, B. Wasylyk, Head and neck squamous cell carcinoma transcriptome analysis by comprehensive validated differential display, Oncogene 25 (2006) 1821–1831.
[15] Y.C. Liao, S.H. Lo, Deleted in liver cancer-1 (DLC-1): a tumor suppressor not just for liver, Int. J. Biochem. Cell Biol. 40 (2008) 843–847.
[16] M.E. Durkin, V. Ullmannova, M. Guan, N.C. Popescu, Deleted in liver cancer 3 (DLC-3), a novel Rho GTPase-activating protein, is downregulated in cancer and inhibits tumor cell growth, Oncogene 26 (2007) 4580–4589.
[17] Y. Gen, K. Yasui, K. Zen, T. Nakajima, K. Tsuji, M. Endo, H. Mitsuyoshi, M. Minami, Y. Itoh, S. Tanaka, M. Taniwaki, S. Arii, T. Okanoue, T. Yoshikawa, A novel amplification target, ARHGAP5, promotes cell spreading and migration by negatively regulating RhoA in Huh-7 hepatocellular carcinoma cells, Cancer Lett. 275 (2009) 27–34.
[18] A. Jemal, F. Bray, M.M. Center, J. Ferlay, E. Ward, D. Forman, Global cancer statistics, CA Cancer J. Clin. 61 (2011) 69–90.
[19] M.M. Shen, C. Abate-Shen, Molecular genetics of prostate cancer: new prospects for old challenges, Genes Dev. 24 (2010) 1967–2000.
[20] J.W. Chiao, B.S. Moonga, Y.M. Yang, R. Kancherla, A. Mittelman, J.R. Wu-Wong, T. Ahmed, Endothelin-1 from prostate cancer cells is enhanced by bone contact which blocks osteoclastic bone resorption, Br. J. Cancer 83 (2000) 360–365.
[21] A. Lopergolo, N. Zaffaroni, Biomolecular markers of outcome prediction in prostate cancer, Cancer 115 (2009) 3058–3067.
[22] F.M. Vega, G. Fruhwirth, T. Ng, A.J. Ridley, RhoA and RhoC have distinct roles in migration and invasion by acting through different targets, J. Cell Biol. 193 (2011) 655–665.
[23] K.J. Livak, T.D. Schmittgen, Analysis of relative gene expression data using real-time quantitative PCR and the 2(−Delta Delta C(T)) method, Methods 25 (2001) 402–408.
[24] A. Takesono, S.J. Heasman, B. Wojciak-Stothard, R. Garg, A.J. Ridley, Microtubules regulate migratory polarity through Rho/ROCK signaling in T cells, PLoS One 5 (2010) e8774.
[25] V.G. Tusher, R. Tibshirani, G. Chu, Significance analysis of microarrays applied to the ionizing radiation response, Proc. Natl. Acad. Sci. U. S. A. 98 (2001) 5116–5121.
[26] S. Gotz, J.M. Garcia-Gomez, J. Terol, T.D. Williams, S.H. Nagaraj, M.J. Nueda, M. Robles, M. Talon, J. Dopazo, A. Conesa, High-throughput functional annotation and data mining with the Blast2GO suite, Nucleic Acids Res. 36 (2008) 3420–3435.
[27] F. van Zijl, G. Krupitza, W. Mikulits, Initial steps of metastasis: cell invasion and endothelial transmigration, Mutat. Res. 728 (2011) 23–34.
[28] N. Reymond, P. Riou, A.J. Ridley, Rho GTPases and cancer cell transendothelial migration, Methods Mol. Biol. 827 (2012) 123–142.
[29] S. Xie, M. Zhu, G. Lv, Q. Zhang, G. Wang, The role of RhoC in the proliferation and apoptosis of hepatocellular carcinoma cells, Med. Oncol. 29 (2012) 1802–1809.
[30] A. Faried, L.S. Faried, H. Kimura, M. Nakajima, M. Sohda, T. Miyazaki, H. Kato, N. Usman, H. Kuwano, RhoA and RhoC proteins promote both cell proliferation and cell invasion of human oesophageal squamous cell carcinoma cell lines in vitro and in vivo, Eur. J. Cancer 42 (2006) 1455–1465.
[31] L. Wang, L. Yang, Y. Luo, Y. Zheng, A novel strategy for specifically down-regulating individual Rho GTPase activity in tumor cells, J. Biol. Chem. 278 (2003) 44617–44625.
[32] A. Bagnato, M. Loizidou, B.R. Pflug, J. Curwen, J. Growcott, Role of the endothelin axis and its antagonists in the treatment of cancer, Br. J. Pharmacol. 163 (2011) 220–233.
[33] L.D. Papsidero, M. Kuriyama, M.C. Wang, J. Horoszewicz, S.S. Leong, L. Valenzuela, G.P. Murphy, T.M. Chu, Prostate antigen: a marker for human prostate epithelial cells, J. Natl. Cancer Inst. 66 (1981) 37–42.
[34] S. Araki, Y. Omori, D. Lyn, R.K. Singh, D.M. Meinbach, Y. Sandman, V.B. Lokeshwar, B.L. Lokeshwar, Interleukin-8 is a molecular determinant of androgen independence and progression in prostate cancer, Cancer Res. 67 (2007) 6854–6862.
[35] M. Saleem, V.M. Adhami, W. Zhong, B.J. Longley, C.Y. Lin, R.B. Dickson, S. Reagan-Shaw, D.F. Jarrard, H. Mukhtar, A novel biomarker for staging human prostate adenocarcinoma: overexpression of matriptase with concomitant loss of its inhibitor, hepatocyte growth factor activator inhibitor-1, Cancer Epidemiol. Biomarkers Prev. 15 (2006) 217–227.
[36] P. Laidler, J. Dulinska, M. Lekka, J. Lekki, Expression of prostate specific membrane antigen in androgen-independent prostate cancer cell line PC-3, Arch. Biochem. Biophys. 435 (2005) 1–14.

[37] A.G. Banerjee, J. Liu, Y. Yuan, V.K. Gopalakrishnan, S.L. Johansson, A.K. Dinda, N.P. Gupta, L. Trevino, J.K. Vishwanatha, Expression of biomarkers modulating prostate cancer angiogenesis: differential expression of annexin II in prostate carcinomas from India and USA, Mol. Cancer 2 (2003) 34.
[38] M.G. Dozmorov, R.E. Hurst, D.J. Culkin, B.P. Kropp, M.B. Frank, J. Osban, T.M. Penning, H.K. Lin, Unique patterns of molecular profiling between human prostate cancer LNCaP and PC-3 cells, Prostate 69 (2009) 1077–1090.
[39] K. Kaibuchi, S. Kuroda, M. Amano, Regulation of the cytoskeleton and cell adhesion by the Rho family GTPases in mammalian cells, Annu. Rev. Biochem. 68 (1999) 459–486.
[40] E. Sahai, C.J. Marshall, ROCK and Dia have opposing effects on adherens junctions downstream of Rho, Nat. Cell Biol. 4 (2002) 408–415.
[41] K.J. Simpson, A.S. Dugan, A.M. Mercurio, Functional analysis of the contribution of RhoA and RhoC GTPases to invasive breast carcinoma, Cancer Res. 64 (2004) 8694–8701.
[42] K.A. Dietrich, R. Schwarz, M. Liska, S. Grass, A. Menke, M. Meister, G. Kierschke, C. Langle, F. Genze, K. Giehl, Specific induction of migration and invasion of pancreatic carcinoma cells by RhoC, which differs from RhoA in its localisation and activity, Biol. Chem. 390 (2009) 1063–1077.
[43] D.I. Bellovin, K.J. Simpson, T. Danilov, E. Maynard, D.L. Rimm, P. Oettgen, A.M. Mercurio, Reciprocal regulation of RhoA and RhoC characterizes the EMT and identifies RhoC as a prognostic marker of colon carcinoma, Oncogene 25 (2006) 6959–6967.
[44] A. Schmidt, A. Hall, Guanine nucleotide exchange factors for Rho GTPases: turning on the switch, Genes Dev. 16 (2002) 1587–1609.
[45] R.I. Bustos, M.A. Forget, J.E. Settleman, S.H. Hansen, Coordination of Rho and Rac GTPase function via p190B RhoGAP, Curr. Biol. 18 (2008) 1606–1611.
[46] H. Xu, S. Eleswarapu, H. Geiger, K. Szczur, D. Daria, Y. Zheng, J. Settleman, E.F. Srour, D.A. Williams, M.D. Filippi, Loss of the Rho GTPase activating protein p190-B enhances hematopoietic stem cell engraftment potential, Blood 114 (2009) 3557–3566.
[47] N. Tatsis, D.A. Lannigan, I.G. Macara, The function of the p190 Rho GTPase-activating protein is controlled by its N-terminal GTP binding domain, J. Biol. Chem. 273 (1998) 34631–34638.
[48] W.T. Arthur, K. Burridge, RhoA inactivation by p190RhoGAP regulates cell spreading and migration by promoting membrane protrusion and polarity, Mol. Biol. Cell 12 (2001) 2711–2720.
[49] Y. Kawanabe, S.M. Nauli, Endothelin, Cell. Mol. Life Sci. 68 (2011) 195–203.
[50] J. Nelson, A. Bagnato, B. Battistini, P. Nisen, The endothelin axis: emerging role in cancer, Nat. Rev. Cancer 3 (2003) 110–116.
[51] J.B. Nelson, S.P. Hedican, D.J. George, A.H. Reddi, S. Piantadosi, M.A. Eisenberger, J.W. Simons, Identification of endothelin-1 in the pathophysiology of metastatic adenocarcinoma of the prostate, Nat. Med. 1 (1995) 944–949.
[52] E.S. Kopetz, J.B. Nelson, M.A. Carducci, Endothelin-1 as a target for therapeutic intervention in prostate cancer, Invest. New Drugs 20 (2002) 173–182.
[53] M.A. Carducci, R.J. Padley, J. Breul, N.J. Vogelzang, B.A. Zonnenberg, D.D. Daliani, C.C. Schulman, A.A. Nabulsi, R.A. Humerickhouse, M.A. Weinberg, J.L. Schmitt, J.B. Nelson, Effect of endothelin-A receptor blockade with atrasentan on tumor progression in men with hormone-refractory prostate cancer: a randomized, phase II, placebo-controlled trial, J. Clin. Oncol. 21 (2003) 679–689.
[54] M.D. Michaelson, D.S. Kaufman, P. Kantoff, W.K. Oh, M.R. Smith, Randomized phase II study of atrasentan alone or in combination with zoledronic acid in men with metastatic prostate cancer, Cancer 107 (2006) 530–535.
[55] J.B. Nelson, Endothelin inhibition: novel therapy for prostate cancer, J. Urol. 170 (2003) S65–S67, (discussion S67-68).
[56] D. Lagares, O. Busnadiego, R.A. Garcia-Fernandez, S. Lamas, F. Rodriguez-Pascual, Adenoviral gene transfer of ET-1 in the lung induces pulmonary fibrosis through FAK activation, Am. J. Respir. Cell Mol. Biol. 47 (2012) 834–842.
[57] K. Mori, M. Amano, M. Takefuji, K. Kato, Y. Morita, T. Nishioka, Y. Matsuura, T. Murohara, K. Kaibuchi, Rho-kinase contributes to sustained RhoA activation through phosphorylation of p190A RhoGAP, J. Biol. Chem. 284 (2009) 5067–5076.
[58] L. Rosano, R. Cianfrocca, S. Masi, F. Spinella, V. Di Castro, A. Biroccio, E. Salvati, M.R. Nicotra, P.G. Natali, A. Bagnato, Beta-arrestin links endothelin A receptor to beta-catenin signaling to induce ovarian cancer cell invasion and metastasis, Proc. Natl. Acad. Sci. U. S. A. 106 (2009) 2806–2811.